

Investigation on the performance of an aerostatic spindle with consideration of fluid-structure-thermal interaction effect

Qiang Gao^{1,2}, Lihua Lu¹, Wanqun Chen^{1,2}, Guanglin Wang¹, Dehong Huo²

¹School of Mechatronics Engineering, Harbin Institute of Technology, Harbin, 150001, China

²School of Engineering, Newcastle University, Newcastle upon Tyne, NE1 7RU, UK

gaoqhhit@gmail.com

Abstract

The performance of aerostatic spindle is significantly affected by the fluid-structure-thermal interaction (FSTI) between the air film, the solid structure and the temperature field of spindle system. In this study, a novel simulation model of aerostatic spindle system is proposed to investigate the FSTI of the aerostatic spindle system, by which the elastic deformation and the thermal deformation of solid component can be considered simultaneously to estimate the performance of aerostatic bearing. Besides, the variation of the performance of air bearing and the gravitational eccentricity of shaft during the temperature rising process can also be obtained, which provides insight into the FSTI phenomenon of aerostatic spindle. Finally, the accuracy of simulation results are verified by testing the time-varying temperature of aerostatic spindle system.

Aerostatic spindle; air bearing; fluid-structure-thermal interaction; thermal behaviour

1. Introduction

Aerostatic spindles are widely adopted in ultra-precision machining equipment owing to their distinct merits of high speed, negligible friction and excellent rotation accuracy. The performance of spindle influences the machining accuracy significantly. In actual working condition, both the elastic deformation of solid structure induced by air film and the thermal deformation caused by temperature raise has a dramatic impact on the overall performance of machine tool and its machining accuracy.^[1-2] It is therefore required to have a comprehensive understanding on the FSTI of air spindle.

In this paper, the FSTI phenomenon is theoretically and experimentally investigated. Firstly, a comprehensive FSTI modeling method is proposed, and the FSTI model of an air spindle is built as case study. Then, the variation of the performance of air bearing and the gravitational eccentricity of shaft during the temperature rising process of air spindle can be obtained, which provides insight for the FSTI behavior of air spindle. Finally, the simulation results are verified by testing the time-varying temperature of air spindle.

2. A comprehensive FSTI modelling method

The actual air film thickness can be calculated by Eq.(1)

$$h_t = h_0 - \Delta h_d - \Delta h_e - \Delta h_t \quad (1)$$

Where h_t is the air film thickness when $t=t_i$, h_0 is the initial air film thickness, Δh_d is the change of air film thickness induced by elastic deformation of solid components, Δh_e is the change of air film thickness due to the weight of rotating parts, Δh_t is the change of air film thickness caused by thermal deformation of solid components. Δh_d , Δh_e and Δh_t can be acquired by solving the thermoelastic motion equations of solid structure based on FEM as shown in Eq.(2).

$$\begin{bmatrix} [M] & [0] \\ [0] & [0] \end{bmatrix} \begin{Bmatrix} \{\ddot{u}\} \\ \{\ddot{T}\} \end{Bmatrix} + \begin{bmatrix} [C] & [0] \\ [0] & [C^*] \end{bmatrix} \begin{Bmatrix} \{\dot{u}\} \\ \{\dot{T}\} \end{Bmatrix} + \begin{bmatrix} [K] & [K^*] \\ [0] & [K^*] \end{bmatrix} \begin{Bmatrix} \{u\} \\ \{T\} \end{Bmatrix} = \begin{Bmatrix} \{F\} \\ \{Q\} \end{Bmatrix} \quad (2)$$

Where $[M]$, $[C]$ and $[K]$ represent the mass matrix, structural damping matrix and stiffness matrix, respectively, and $\{u\}$ is the displacement vector. $\{F\}$ represents the sum of the force vectors, $\{Q\}$ represents the sum of the heat generation load and convection surface heat flow vectors. $[C^*]$ is the thermoelastic damping matrix, $[C^*]$ is the specific heat matrix. $[K^*]$ is the thermal conductivity matrix, $[K^*]$ is the thermoelastic stiffness matrix. $[T]$ is the temperature vector. The air film force applied on solid components can be acquired by calculating the governing equations of fluid domain, as shown in Eq.(3)-(4). The heat generation of motor, the fluid-structure conjugate heat transfer, and convection heat transfer of air spindle can be simulated by the energy equation, as shown in Eq.(5).

$$\frac{\partial \rho}{\partial t} + \nabla \cdot (\rho \vec{v}) = 0 \quad (3)$$

$$\frac{\partial}{\partial t} (\rho \vec{v}) + \nabla \cdot (\rho \vec{v} \vec{v}) = -\nabla p + \nabla \cdot (\vec{\tau}) \quad (4)$$

$$\frac{\partial (\rho E)}{\partial t} + \nabla \cdot (\vec{v} (\rho E + p)) = \nabla \cdot (k \nabla T + (\vec{\tau} \cdot \vec{v})) + S_h \quad (5)$$

Where ρ indicates the density, \vec{v} is the velocity vector. p indicates the pressure. k is the conductivity. T is the temperature. $\vec{\tau}$ is the stress tensor. E is the energy content per unit mass. The term S_h is the volumetric heat source, such as the energy caused by iron loss of the motor. The term $\nabla \cdot (\vec{\tau} \cdot \vec{v})$ is the energy caused by the viscous dissipation of air film. The term $\nabla \cdot (k \nabla T)$ represents the heat transfers among the solid components, fluid domain of air film and ambient air due to thermal conduction and thermal convection.

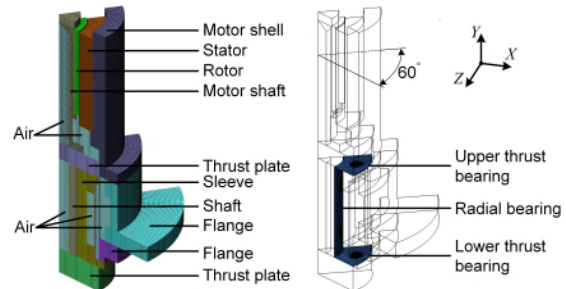


Figure 1. The FSTI model of aerostatic spindle system

Therefore, Eq.(1)-(5) are the mathematical model of FSTI modelling method. They are solved by combing the FEM software ANSYS and CFD software Fluent. Figure 1 demonstrates the computational mesh of the FSTI model of air spindle system. To save calculation time, a basic sector which represents one sixth of aerostatic spindle system is built due to the aerostatic spindle system is cyclically symmetric.

3. The calculation results of proposed FSTI model

The temperature rising process of air spindle at rotation speed of 2000rpm is demonstrated in Figure 2. Figure 2(a) shows the temperature distribution of air spindle at $T_m=18000s$. It shows that the temperature field of air spindle is nonuniform. The maximum temperature of air spindle reaches $33.6^{\circ}C$, and the minimum temperature is $25.8^{\circ}C$. Figure 2(b) presents the temperature curves of four points. The locations of these four points are marked in Figure 2(a). It can be seen that the temperature curves of these four points first increase sharply, and then their slopes decrease gradually. The temperatures of points 1 and 2 are much higher than that of points 3 and 4 due to points 1 and 2 are closer to the motor stator.

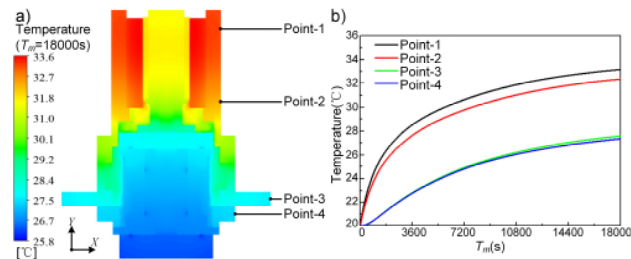


Figure 2. Temperature rising process of aerostatic spindle system

Figure 3 illustrates the deformation process of aerostatic spindle acquired by FSTI model. Figure 3(a) shows the axial displacement of aerostatic spindle system when $T_m=18000s$. To quantitatively analyze the structural deformation and air film thickness change, six points are marked are shown in Figure 3(a), and their axial displacements-time curves are compared in Figure 3(b). Point 5 and point 9 are located at the top and bottom of shaft, respectively. While, point 6 and point 8 are located at the top and bottom of sleeve, respectively. Point 7 is at the middle of shaft, and point 10 locate at the bottom of thrust plate.

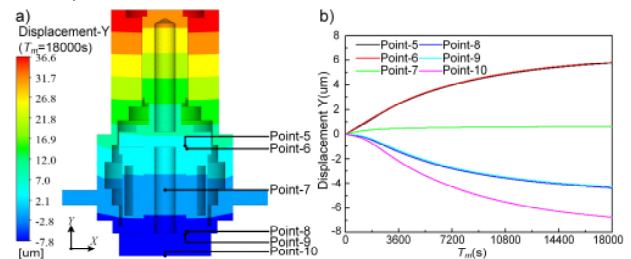


Figure 3. Deformation process of aerostatic spindle system

As shown in Figure 3(b), the displacements of each points show different behaviors. It shows that the displacement of point 6 is larger than that of point 5, and the displacement of point 8 is larger than point 9. Hence, both the upper and lower air film thickness decrease gradually with the continuous deformation of air spindle. The displacement curve of point 7 indicates that the axial position of shaft is also slightly moved during the deformation process. The axial position of shaft is determined by the balance between air film forces and gravity of rotating parts. Hence, the axial position change of shaft can

represent the change of gravitational eccentricity. The displacement of point 10 represents the axial thermal error of air spindle. It is mainly derived from the thermal expansion of shaft and thrust plate.

The change of air film thickness of air film will cause the change of air bearing performance. Figure 4 demonstrates the time-varying air film forces of air bearings. As shown in Figure 4, both the upper and lower air film force ascend slightly. It is because of that the air film force of air thrust bearing increase with the decline of air film thickness. As the average air film thickness of upper and lower air films decline due to thermal deformation, therefore their air film forces increase. Besides, the difference between upper and lower air film forces keeps constant, which is equal to the gravity of rotating parts.

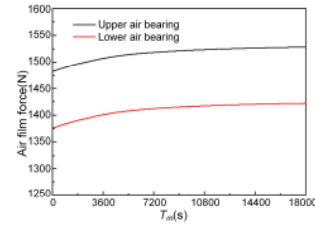


Figure 4. Variation of the performance of aerostatic bearings

4. Experiment

To verify the accuracy of proposed comprehensive FSTI model method, the temperature variation of aerostatic spindle is measured in this section. The experimental setup is shown in Figure 5(a). The experimental apparatus consists of computer, temperature sensors and aerostatic spindle. The locations of temperature sensors are demonstrated in Figure 5(a). To eliminate the influence from room temperature changing, the test setup is placed in a temperature-controlled room. And before testing, the air spindle is placed in the temperature-controlled room for 24 hours with room temperature of $20^{\circ}C$.

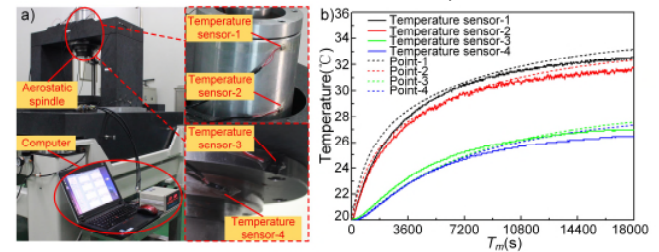


Figure 5. Experiment setup and tested results

The experiments are carried out with air supply pressure at 0.5MPa, rotational speed of 2000rpm, and room temperature of $20^{\circ}C$. Figure 5(b) shows the measured temperature curves of each sensors. Comparing with the simulation results, it shows that the measured data agree well with the simulated results, which proves the reliability of simulation results.

5. Conclusion

This paper investigates the influence of FSTI phenomenon on the performance of aerostatic spindle. A comprehensive FSTI modeling method is proposed, and further verified by experiments. The FSTI phenomenon of an aerostatic spindle system is investigated as a case study, which provides insight to understand the FSTI phenomenon.

References

- [1] Gao Q, Lu L, Chen W, Guoda Chen, Guanglin Wang 2017 *Tribol Int.* 115:461-469.

- [2] Gao S, Cheng K, Ding H, Hongya Fu 2015 *Proc I MechE Part J: J Engineering Tribology*. **230**(7):852-871.